miR-129-5p inhibits oxidized low-density lipoprotein-induced A7r5 cell viability and migration by targeting HMGB1 and the PI3k/Akt signaling pathway

HONGFEI JIANG, REN GONG and YANQING WU

Department of Cardiology, The Second Affiliated Hospital of Nanchang University, Nanchang, Jiangxi 330006, P.R. China

Received November 17, 2020; Accepted August 17, 2021

DOI: 10.3892/etm.2022.11168

Abstract. The mechanisms underlying gene therapy for the treatment of cardiovascular diseases remain to be elucidated. microRNAs (miRs) have been recognized as key regulators in vascular smooth muscle cells, which are involved in the formation of atherosclerosis. The present study aimed to explore the role of miR-129-5p in the regulation of high-mobility group box 1 protein (HMGB1) and the PI3k/Akt signaling pathway, and further explore the role of miR-129-5p in the viability and migration of A7r5 cells induced by oxidized low-density lipoprotein (ox-LDL). Cell viability, viability and migration were determined using Cell Counting Kit-8, colony formation, wound healing and Transwell assays. The expression levels of miR-129-5p and HMGB1 were detected using reverse transcription-quantitative PCR and western blotting. A dual-luciferase assay was used to confirm the association between miR-129-5p and HMGB1. RT-qPCR results in the present study demonstrated that the expression levels of miR-129-5p in A7r5 cells induced by ox-LDL were significantly decreased, compared with the control cells. Moreover, the viability and migration of A7r5 cells induced by ox-LDL were increased compared with control group. Western blot and RT-qPCR results showed that miR-129-5p decreased the expression of HMGB1 in A7r5 cells compared with control group. The present results demonstrated that miR-129-5p inhibited the viability, viability and migration of A7r5 cells induced by ox-LDL, and directly targeted HMGB1 to regulate the PI3k/Akt signaling pathway. In conclusion, miR-129-5p inhibited the PI3k/Akt signaling pathway by directly targeting HMGB1, and reduced the viability, viability and migration of A7r5 cells induced by ox-LDL.

Correspondence to: Professor Yanqing Wu, Department of Cardiology, The Second Affiliated Hospital of Nanchang University, 1 Minde Road, Nanchang, Jiangxi 330006, P.R. China
E-mail: wuyanqing01@sina.com

Key words: microRNA-129-5p, A7r5 cells, high-mobility group box 1 protein, viability

Introduction

Cardiovascular disease (CVD) is a leading cause of mortality worldwide (1). One of the main causes of CVD is atherosclerosis (AS) (2), and the pathological mechanisms underlying AS have been the focus of a number of studies. AS is recognized as a chronic arterial inflammatory disease that is induced by oxidized low-density lipoprotein (ox-LDL) accumulation and inflammation of the arterial intima under hypercholesterolemic conditions (3). The results of previous pharmacological studies have demonstrated that the main risk factors of AS include dyslipidemia, hypertension, alcohol consumption, smoking, diabetes, obesity and a lack of exercise (4). Currently, dyslipidemia is considered the most critical risk factor of AS (5). Ox-LDL is a critical diagnostic marker of AS (6), and has the ability to cause lipid metabolism disorders, promote the formation of foam cells derived from vascular smooth muscle cells (VSMCs), and regulate the proliferation, apoptosis, migration and differentiation of VSMCs, which serve vital roles in the development of AS (7).

The results of previous studies have revealed the key signals and molecular pathways (e.g., MAPK/ERK, Nrf2) underlying the formation and development of atherosclerotic plaques (8,9). Moreover, the role of microRNAs (miRNAs/miRs) in CVD have remained the focus of a number of studies. miRNAs are a family of highly conserved, endogenous non-coding small RNA molecules that regulate gene expression through binding of the 3'-untranslated region (3'-UTR) of target mRNAs (10-12). miRNAs are involved in diverse cellular functions, including differentiation, growth, proliferation, migration, senescence and apoptosis in a number of cells including cancer cells, HUVECs and H9c2 (13). Moreover, A previous study demonstrated that miRNAs serve essential roles in regulating AS (14). Geng *et al* (14) reported that ox-LDL increased the expression levels of miR-129-5p in human aortic endothelial cells, thereby decreasing cell proliferation. This led to a decrease in the mRNA expression of Beclin-1, which decreased endothelial cell autophagy in AS. Thus, miR-129-5p exerted differing effects on a number

of cells under the pathological conditions of AS, which is dependent on the targeted cell type (8). The results of previous studies have provided novel molecular insights into the impact of miRNAs in AS pathways, identifying them as novel therapeutic targets. For example, miR-181b acts as an inhibitor of endothelial inflammatory responses by targeting NF-κB binding in AS (15). The results of an study demonstrated the role of miR-221/miR-222 in the regulation of platelet derived growth factor-mediated VSMC proliferation (16). Moreover, miR-145 served a regulative role in aberrant VSMC proliferation, which is a key pathological process of AS (17). Liu *et al* (18) demonstrated the role of miR-21 as a key target for protective reagents against ox-LDL-induced rat vascular endothelial cell injury, which may serve critical roles in the development of AS (18). Furthermore, miR-129-5p has been demonstrated to suppress carcinogenesis in a number of cancers including gastric cancer and osteoscarcoma (19,20). However, the specific role of miR-129-5p in the development of AS is yet to be fully elucidated.

High-mobility group box 1 protein (HMGB1), a highly conserved and widely expressed DNA-binding protein, is a key mediator of cell migration and proliferation (21). Notably, the results of a previous study demonstrated that HMGB1 was overexpressed in cancer cells and promoted cell invasion and migration (22). HMGB1 has been reported to participate in the regulation of AS progression. For example, Wu *et al* (23) demonstrated that miR-328 mitigated ox-LDL-induced endothelial cell injury by targeting HMGB1 in AS. Moreno *et al* (24) also reported that HMGB1 was highly expressed in atherosclerotic plaques.

In the present study, ox-LDL-induced A7r5 cells were used to determine the role of miR-129-5p in cell migration and proliferation, and to investigate the association of miR-129-5p with HMGB1 and the PI3k/Akt signaling pathway.

Materials and methods

Materials. FBS, bovine serum albumin (BSA) and endothelial cell growth supplement were purchased from Gibco; Thermo Fisher Scientific, Inc. Ox-LDL was purchased from Unionbiol. Cell Counting Kit-8 (CCK-8) was purchased from Dojindo Molecular Technologies, Inc. (cat. no. CK04).

Cell culture. A7r5 cells were purchased from The American Type Culture Collection and maintained in DMEM (Gibco; Thermo Fisher Scientific, Inc.) containing 10% FBS (Gibco; Thermo Fisher Scientific, Inc.), 1 mmol/l sodium pyruvate, 4 mmol/l L-glutamine, 4.5 g/l glucose, 1.5 g/l sodium bicarbonate, 100 mg/ml streptomycin and 100 U/ml penicillin at 37˚C in a humidified atmosphere with 5% CO_2.

Cell transfection. A7r5 cells were transfected with 20 nM miR-129-5p mimics (5'CUUUUUGCGGUCUGGGCU UGC3') or the corresponding negative control (Shanghai GenePharma Co., Ltd.) using Lipofectamine® 2000 reagent (Invitrogen; Thermo Fisher Scientific, Inc.) for 48 h at 37˚C. For HMGB1 overexpression, the recombinant sense expression vector plasmid Cytomegalovirus promoter DNA 3.1 for HMGB1 (1 μg/μl pcDNA3.1-HMGB1; Invitrogen; Thermo Fisher Scientific, Inc.) was constructed by subcloning the cDNA fragment of HMGB1 containing the complete coding sequence between *Kpn*I and *Bam*HI. Cells were transfected using Lipofectamine® 2000 according to the manufacturer's protocol. Cells in the control group were transfected with pcDNA3.1-NC (empty vector). Following transfection, cells were incubated with fresh DMEM for 24 h, the medium was replaced with fresh and cells were incubated for a further 24 h at 37˚C. Cells were collected for subsequent experiments.

Wound healing. A7r5 cells were cultured in six-well culture plates ($1x10^6$ cells/well) for 48 h at 37˚C. The wound healing assay was conducted as previously described (25). The cell monolayers on the surface of the six-well plate were scratched with a 200 μl micropipette tip. Cells were subsequently incubated at 37˚C for 24 h in DMEM containing 2% FBS (26). Non-adherent cells were washed with PBS and the remaining cells were treated with ox-LDL (0, 10, 20 and 40 μg/ml) based on preliminary experiments. Images were captured using light microscope (magnification, x40), and images of linear wounds were obtained from nine fields/well at 0 and 48 h after injury. Three independent repeats were carried out.

CCK-8 assays for the detection of cell viability. Cell viability was assessed using a CCK-8 assay kit. A7r5 cells were cultured in 96-well plates overnight at a density of 10^4 cells/well at 37˚C, and subsequently transfected with miR-129-5p mimics or an inhibitor as previously described. At 48 h after transfection, 10 μl CCK-8 solution was added to each well for 1 h and absorbance readings at 450 nm were obtained in triplicate using a spectrophotometric plate reader. Three wells were measured for each data point and three independent repeats were conducted.

Transwell migration assay. A total of $1x10^5$ A7r5 cells were collected and seeded in a six-well plate. After the cells had attached, they were treated with ox-LDL at 0, 10, 20, 40 μg/ml for 48 h. The cells were collected and 5,000 cells/well in 200 μl/well were seeded into the upper chambers filled DMEM without FBS that had been pre-coated with 150 mg Matrigel (BD Biosciences) 24 h at 37˚C for invasion assays. The lower chambers were filled with DMEM containing 10% FBS. Following incubation at 37˚C for 48 h, cells remaining on the upper surface of the membrane were removed. Cells on the lower surface of the membrane were fixed with 4% paraformaldehyde and stained with 0.1% crystal violet for 15 min at room temperature. Stained cells were subsequently observed and counted under a light microscope (magnification, x100). Three independent experiments were performed.

Colony formation assay. A7r5 cells were treated with ox-LDL (0, 10, 20 and 40 μg/ml), seeded in 60-mm plates at 1,000 cells/well and the culture was terminated when colonies became visible to the naked eye and contained >50 cells. The cells were washed with 1X PBS, fixed in 4% paraformaldehyde for 15 min and stained with 0.1% (w/v) Giemsa at room temperature. Colonies were subsequently viewed and counted

in 10 randomly selected fields under a light microscope magnification, x100, Nikon Corporation), and images were captured using a digital camera (Canon Inc.). The percentage of colony formation for each group was calculated using the following equation: Percentage of colony formation (%)=the number of colonies/1,000 x100. Three independent experiments were performed.

Bioinformatics analysis. Bioinformatics analysis was performed to predict the downstream miRNA that would interact with HMGB1, to further investigate the regulatory mechanism of miR129-5p. TargetScan (http://www.targetscan.org/vert_72/) and miRBase (https://www.mirbase.org/) were used for the gene prediction, according to the online software operating instructions.

RNA isolation and reverse transcription-quantitative (RT-q) PCR for miR-129-5p. A total of 1 μg RNA was extracted from A7r5 cells using TRIzol® reagent (Thermo Fisher Scientific, Inc.). Reverse transcription was performed using RT Reagent kit (cat. no. RR037A; Takara, Bio, Inc.). qPCR (cat. no. RR820A; Takara, Bio, Inc.) was performed using SYBR Green mix (Takara Bio, Inc.) with primers specific to miR-129-5p (Guangzhou RiboBio Co., Ltd.). The PCR conditions were as follows: 95˚C for 10 min, followed by 40 cycles at 95˚C for 30 sec, 60˚C for 30 sec and 72˚C for 1 min. Relative quantification of the miRNA expression was calculated using the $2^{-\Delta\Delta Cq}$ method (27). The sequence of miR-129-5p was: 5'CUUUUUGCGGUCUGGGCUUGC3'. HMGB1, Forward 5'ATCCTGGCTTATCCATTGGTGAT3'; Reverse 5'CTCG TCGTCTTCCTCTTCCTTCT3'. The corresponding PCR primers were: miR-129-5p, Forward 5'-ACACTCCAGCTG GGTCCCTGAGACCCTTAA-3' and Reverse CTCAACTGG TGTGGAGT-; U6, Forward: 5'-CTCGCTTCGGCAGCA CA-3' and Reverse 5'-AACGCTTCACGAAYYYGCGT-3'. U6 was selected as the housekeeping gene to normalize the expression of miR-129-5p.

Dual-luciferase reporter assay. Wild-type (WT) or mutant (MUT) versions of miR-129-5p were subcloned into the pGL3 Basic vector (Promega Corporation). A total of 20 nM miR-129-5p mimics (5'CUUUUUGCGUCUGGGCUUGC3') (Guangzhou RiboBio Co., Ltd.) were co-transfected with pLUC-WT-HMGB1 (5'UACCACUCUGUAAUUGCAAAA AA) or pLUC-MUT-HMGB1 (5'UACCACUCUGUAAUU CCUAUAUA) (500 ng) into $3x10^4$ A7r5 cells. Cells were transfected using Lipofectamine® 2000 (Invitrogen; Thermo Fisher Scientific, Inc.) according to the manufacturer's protocol. After 48 h incubation at 37˚C, the cells were lysed by lysis buffer as supplied by the Dual-Luciferase Detection kit (Beyotime Institute of Biotechnology) on ice and luciferase activity was tested using the Dual-Luciferase Reporter assay system (Promega Corporation). Luciferase activity was normalized to *Renilla* luciferase activity. After transfection for 48 h, relative luminescence was tested using luminometry according to the manufacturer's instructions.

Western blotting assay. Cell lysates from ox-LDL treated A7r5 cells were placed on ice in 1X RIPA lysis buffer (Sigma-Aldrich; Merck KGaA) containing protease and phosphatase inhibitors (Thermo Fisher Scientific, Inc.). The concentration of the protein in cells lysates was detected using a BCA kit (Beijing Solarbio Science & Technology Co., Ltd.). The proteins in cell lysates (10 μg) were separated using SDS-PAGE on a 10% gel. The separated proteins were subsequently transferred onto a nitrocellulose membrane and incubated with 5% non-fat milk solution or 5% BSA for 1 h at room temperature. The membranes were incubated with primary antibodies against HMGB1, focal adhesion kinase (FAK; cat. no. 3285, 1:1,000; Cell Signaling Technology, Inc.), Akt (cat. no. 9272, 1:1,000; Cell Signaling Technology, Inc.), PI3k (cat. no. 4255, 1:1,000; Cell Signaling Technology, Inc.), phosphorylated (p)-FAK (cat. no. 3281, 1:1,000; Cell Signaling Technology, Inc.), p-Akt (cat. no. 9275, 1:1,000; Cell Signaling Technology, Inc.), and GAPDH (cat. no. 5174; 1:1,000, Cell signal Technology, Inc.) at 4˚C overnight. The membrane was washed with TBS-Tween-20 (20%) 3 times (8 min) and subsequently incubated with anti-rabbit IgG (TA354196, 1:10,000) or anti-mouse IgG antibodies (TA35266, 1:10,000; OriGene Technologies, Inc.) conjugated to horseradish peroxidase for 1 h at room temperature. Bands were visualized using an ECL detection kit (Thermo Fisher Scientific, Inc.). Then band intensities were determined using ImageJ software v. 1.4 (National Institutes of Health), and normalized to GAPDH.

Statistical analysis. Each experiment was carried out at least three times, and all values are presented as the mean ± SD. SPSS 22.0 software (IBM Corp.) was used to analyze the data. Comparisons between two means were evaluated using a paired Student's t-test. Comparisons among multiple groups were evaluated using one-way ANOVA followed by Bonferroni's post hoc test. $P<0.05$ was considered to indicate a statistically significant difference.

Results

Ox-LDL increases the viability and migration of A7r5 cells. The viability of A7r5 cells induced by 0, 10, 20 and 40 μg/ml ox-LDL was investigated using CCK-8 and clone formation assays. Following ox-LDL treatment, the results of the CCK-8 assay demonstrated that compared with control group, the absorbance of A7r5 cells significantly increased with the increase of ox-LDL concentration, indicating that ox-LDL increased viability in a dose-dependent manner (Fig. 1A). As presented in Fig. 1, A7r5 cells induced by 40 μg/ml ox-LDL demonstrated the highest level of viability. As exhibited in Fig. 1B, the clone formation of A7r5 cells was significantly increased with the increase of ox-LDL concentration compared with control group, further indicating that ox-LDL increased viability in a dose-dependent manner, and that A7r5 cells induced by 40 μg/ml ox-LDL demonstrated the highest level of viability. Moreover, the results of wound healing and Transwell assays revealed a high level of A7r5 cell migration induced by 40 μg/ml ox-LDL compared with control group (Fig. 1C and D).

miR-129-5p expression levels decrease and HMGB1 expression levels increase in A7r5 cells following treatment with ox-LDL. The results of RT-qPCR demonstrated that the level of miR-129-5p decreased with the increase of ox-LDL

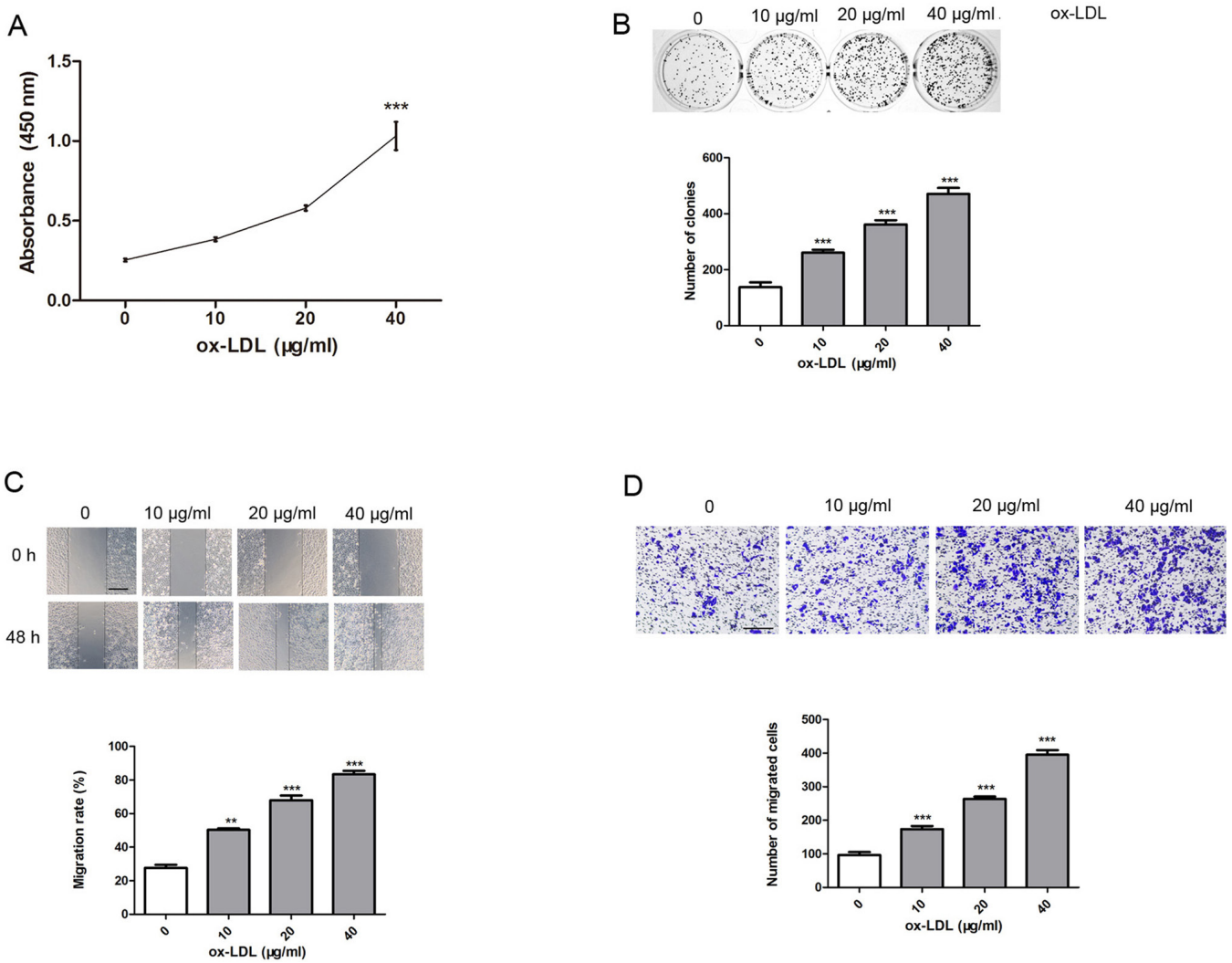

Figure 1. A7r5 cells induced by ox-LDL demonstrate increased viability and migration. (A) Effects of 0, 10, 20 and 40 μg/ml ox-LDL on A7r5 cell viability were measured using a Cell Counting Kit-8 assay. (B) Clonogenicity was detected using a colony formation assay. (C) Wound closure of cells was assessed using a wound healing assay. (D) Migration of cells was performed using a Transwell assay. Scale bars=100 μm. Experiments were repeated three times. **P<0.01 and ***P<0.001 vs. 0 μg/ml ox-LDL. ox-LDL, oxidized low-density lipoprotein.

in A7r5 cells compared with control group. Notably, the expression level of miR-129-5p was the lowest in A7r5 cells following treatment with 40 μg/ml ox-LDL, compared with the control group (Fig. 2A). Furthermore, HMGB1 mRNA and protein expression levels in A7r5 cells induced by 0, 10, 20 and 40 μg/ml ox-LDL were evaluated using western blot analysis and RT-qPCR. As demonstrated in Fig. 2B-D, both HMGB1 protein and mRNA expression levels were the highest in A7r5 cells induced by 40 μg/ml ox-LDL compared with the control group. Thus, the expression levels of HMGB1 were increased, and the expression levels of miR-129-5p were decreased in A7r5 cells following treatment with ox-LDL.

miR-129-5p regulates HMGB1 expression by binding to the HMGB1 3'UTR. Results generated from TargetScan (http://www.targetscan.org/vert_72/) and miRBase (https://www.mirbase.org/) databases suggested that the 3'UTR of HMGB1 contained miR-129-5p seed sites (Fig. 3A). In order to determine whether miR-129-5p directly targeted HMGB1, a dual-luciferase reporter assay was performed after A7r5 cells were co-transfected with HMGB1-WT or HMGB1-MUT reporter plasmids, and either miR-129-5p or miR-NC. The results of the present study demonstrated that miR-129-5p significantly downregulated the luciferase activity of HMGB1-WT plasmid (Fig. 3B), but exerted no notable effects on the activity of the HMGB1-MUT plasmid, indicating that miR129-5p directly targeted HMGB1. RT-qPCR results revealed that the expression levels of miR-129-5p in the miR-129-5p mimics group were significantly increased compared with the mimics control group (Fig. 3C). Moreover, the expression levels of miR-129-5p in the miR-129-5p inhibitor group were significantly reduced compared with the inhibitor control group. Thus, the results of the RT-qPCR analysis confirmed transfection efficiency. In addition, western blotting and RT-qPCR results revealed differences in the expression levels of HMGB1 in miR-129-5p mimics group. As demonstrated in Fig. 3D and E, miR-129-5p downregulated both the HMGB1 mRNA and protein expression levels in A7r5 cells.

miR-129-5p inhibits the viability and migration of A7r5 cells induced by ox-LDL. RT-qPCR was conducted to detect

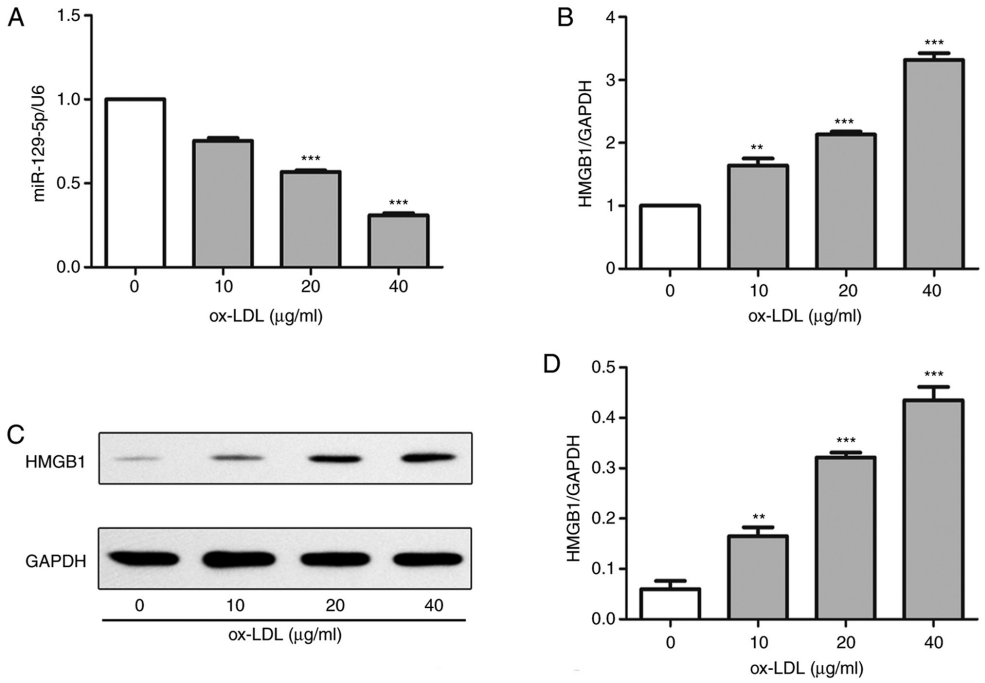

Figure 2. miR-129-5p is downregulated and HMGB1 is upregulated in ox-LDL-induced A7r5 cells. (A) RT-qPCR assays were used to determine the expression levels of miR-129-5p in A7r5 cells following treatment with 0, 10, 20 and 40 μg/ml ox-LDL. (B) RT-qPCR assays were used to determine the expression levels of HMGB1 in A7r5 cells following treatment with 0, 10, 20 and 40 μg/ml ox-LDL. (C) Western blot assays were used to determine the protein expression levels of HMGB1 in A7r5 cells following treatment with 0, 10, 20 and 40 μg/ml ox-LDL. (D) Quantification of HMGB1 protein expression levels in A7r5 cells. Experiments were repeated three times. **P<0.01 and ***P<0.001 vs. 0 μg/ml ox-LDL. miR, microRNA; HMGB1, high-mobility group box 1 protein; ox-LDL, oxidized low-density lipoprotein; RT-qPCR, reverse transcription-quantitative PCR.

the mRNA levels of miR-129-5p in A7r5 cells induced by 0, 10, 20 and 40 μg/ml ox-LDL. The expression levels of miR-129-5p in A7r5 cells induced by 40 μg/ml ox-LDL was significantly reduced compared with the control group (Fig. 4A). Moreover, the expression levels of miR-129-5p were significantly increased in the miR-129-5p mimics group, compared with the ox-LDL group (Fig. 4A). A CCK-8 assay was conducted to analyze the viability of A7r5 cells induced by 40 μg/ml ox-LDL. Notably, the viability of A7r5 cells induced by 40 μg/ml ox-LDL was increased compared with the corresponding control group. However, the viability of A7r5 cells was reduced following transfection with the miR-129-5p mimics and treatment with 40 μg/ml ox-LDL compared with mimics control + 40 g/ml ox-LDL group (Fig. 4B). Furthermore, colony formation and Transwell assays were performed to determine the viability and migration rate of A7r5 cells induced by ox-LDL. The results of the present study demonstrated that the viability and migration of A7r5 cells induced by 40 μg/ml ox-LDL were increased compared with control group. However, the viability and migration of the A7r5 cells were significantly decreased following transfection with the miR-129-5p mimics and treatment with 40 μg/ml ox-LDL compared with 40 μg/ml ox-LDL + mimics control group (Fig. 4C and D).

Effects of miR-129-5p on the viability and migration of A7r5 cells induced by ox-LDL are altered following HMGB1 overexpression. RT-qPCR was conducted to determine HMGB1 mRNA expression levels in A7r5 cells induced by ox-LDL, and in A7r5 cells transfected with miR-129-5p mimics. Notably, the expression level of HMGB1 in the con + miR-129-5p + pcDNA3.1 group was significantly reduced compared with the control group (Fig. 5A). Furthermore, the expression level of HMGB1 was significantly increased in the HMGB1 overexpression group compared with the miR-129-5p mimics group (Fig. 5A). Additionally, the expression level of HMGB1 was markedly increased in the ox-LDL40 + miR-129-5p + pcDNA3.1-HMGB1 group compared with the ox-LDL40 + miR-129-5p + pcDNA3.1 group. A CCK-8 assay was conducted to analyze the viability of A7r5 cells induced by 40 μg/ml ox-LDL. Compared with the control group, the viability of A7r5 cells transfected with miR-129-5p mimics was significantly reduced. Notably, the viability of A7r5 cells induced by 40 μg/ml ox-LDL was significantly increased following HMGB1 overexpression compared with the ox-LDL40 + miR-129-5p + pcDNA3.1 group (Fig. 5B). In order to confirm transfection efficiency, HMGB1 mRNA expression levels were detected using RT-qPCR analysis. The results demonstrated that HMGB1 mRNA expression levels were significantly increased in the con + pcDNA3.1-HMGB1 group compared with the con + pcDNA3.1 group (Fig. 5C). Colony formation and Transwell assays were subsequently performed to determine the viability and migration rates of A7r5 cells induced by ox-LDL. The results of the present study demonstrated that the viability and migration of A7r5 cells induced by 40 μg/ml ox-LDL were increased compared with control group. However, the viability and migration rate of A7r5 cells induced by 40 μg/ml ox-LDL were significantly increased following HMGB1 overexpression

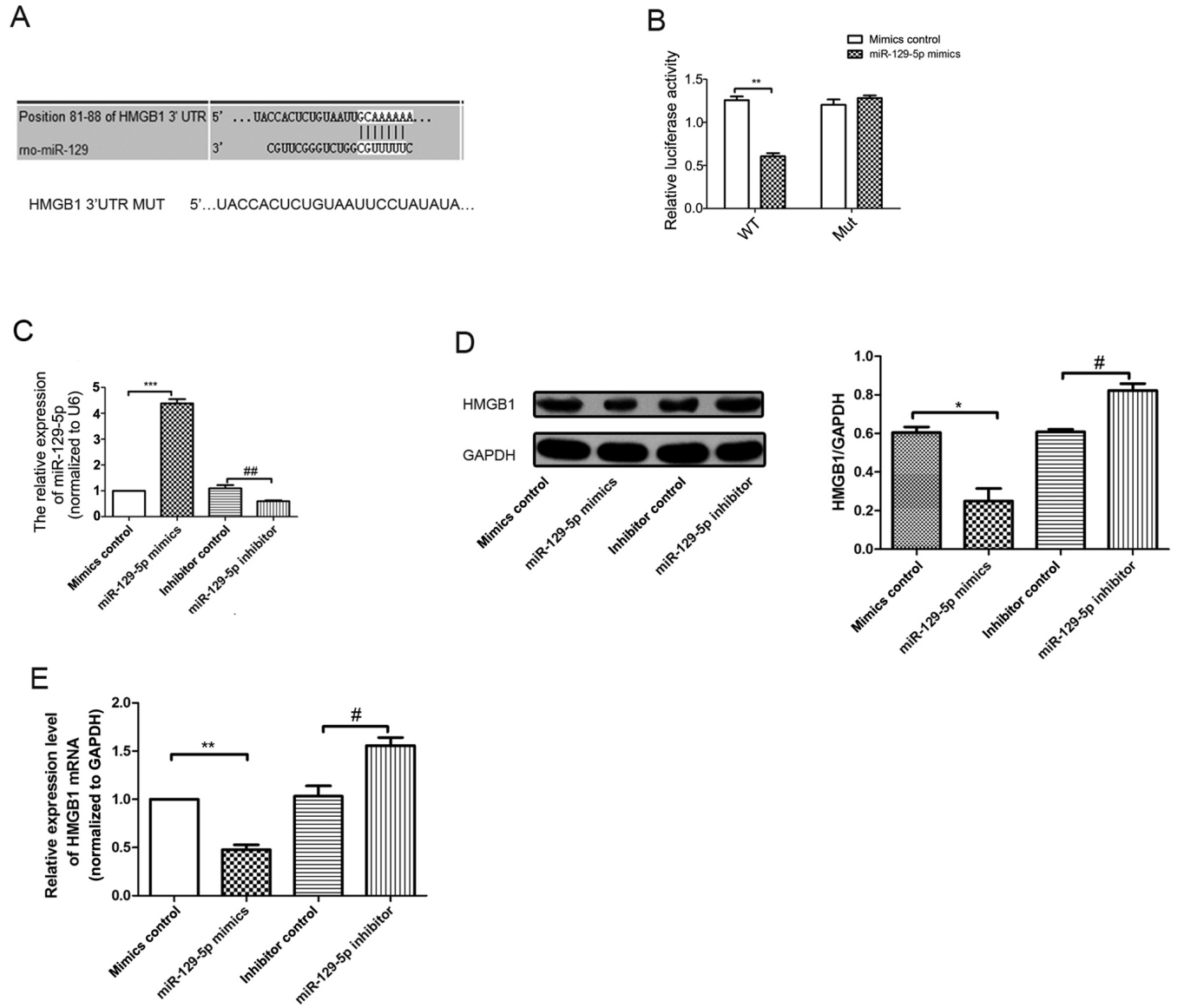

Figure 3. miR-129-5p directly targets HMGB1 in A7r5 cells. (A) Bioinformatics analysis demonstrated that miR-129-5p targets the 3'UTR of HMGB1 mRNA at the specific binding site at 81-88 base pairs. (B) The mutant reporter of HMGB1 was constructed, and A7r5 cells were co-transfected with either miR-129-5p mimics or mimics control. The relative luciferase activity was detected after 48 h. (C) RT-qPCR analysis was used to detect the expression levels of miR-129-5p in different groups (mimics control, miR-129-5p mimics, inhibitor control and miR-129-5p inhibitor). (D) Western blotting analysis was used to detect HMGB1 protein levels following miR-129-5p overexpression in A7r5 cells. (E) mRNA expression levels of HMGB1 in A7r5 cells were detected using RT-qPCR analysis. Experiments were repeated three times. *P<0.05, **P<0.01 and ***P<0.001 vs. mimics control group; $^{\#}$P<0.05 and $^{\#\#}$P<0.01 vs. inhibitor control group. miR, microRNA; HMGB1,high-mobility group box 1 protein; UTR, untranslated region; RT-qPCR, reverse transcription-quantitative PCR; MUT, mutant; WT, wild-type.

compared with 40 μg/ml ox-LDL + pcDNA3.1-NC group (Fig. 5D and E).

Effects of miR-129-5p on the expression and phosphorylation of FAK and Akt. PI3k/Akt-related proteins were investigated in A7r5 cells following transfection with miR-129-5p mimics and treatment with 40 μg/ml ox-LDL. As demonstrated in Fig. 6, the protein expression level of PI3k, along with p-Akt and p-FAK levels were increased in A7r5 cells induced by 40 μg/ml ox-LDL compared with the control group. Moreover, the expression levels of PI3k, and the levels of p-Akt and p-FAK were markedly reduced in A7r5 cells following transfection with the miR-129-5p mimic, compared with A7r5 cells induced by 40 μg/ml ox-LDL (Fig. 6).

Discussion

AS is a main cause of CVDs and cerebrovascular diseases that lead to the highest mortality and morbidity rates worldwide (28). The American Heart Association reported that 17.9 million people died of cardiovascular disease in 2017, accounting for 31 percent of deaths worldwide (29). The main risk factors for AS include hyperglycemia, hyperlipidemia, smoking, poor diet, obesity and diabetes mellitus (30). Epidemiological data have demonstrated that the mortality rate of CVD is much higher than that of other diseases worldwide (31). VSMC proliferation is one of the major contributors to AS, and the associated risk factors remain the focus of current research. For example, ox-LDL

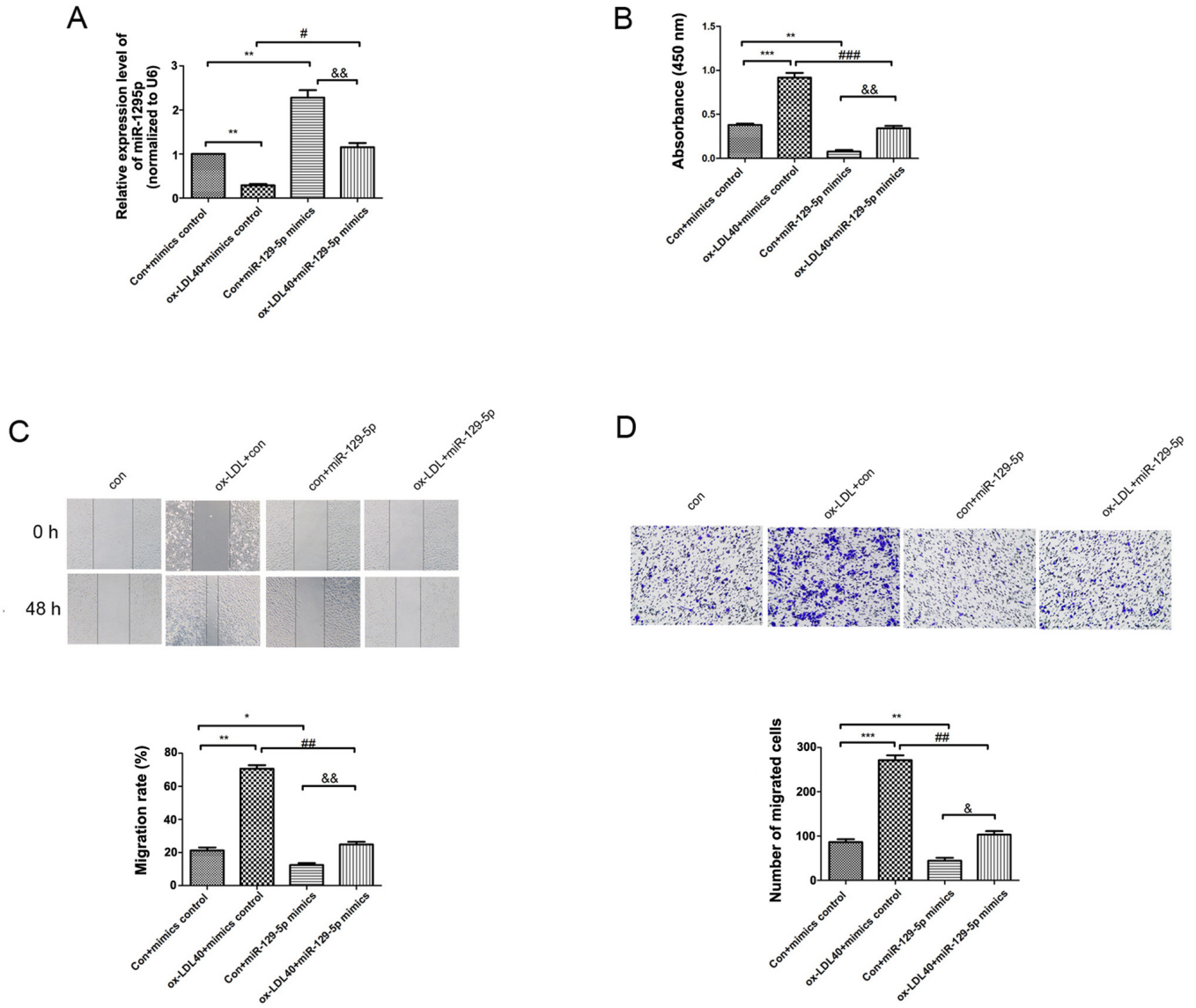

Figure 4. miR-129-5p inhibits the proliferation and migration of ox-LDL-induced A7r5 cells. (A) Reverse transcription-quantitative PCR assays were used to detect the mRNA expression levels of miR-129-5p in A7r5 cells. (B) Cell Counting Kit-8 assays were performed to determine the effects of ox-LDL treatment on A7r5 cell viability. (C) Wound closure of cells was detected using a wound healing assay (magnification, x100). (D) The migration rate of cells was determined using Transwell assays (magnification, x100). Experiments were repeated three times. *P<0.05, **P<0.01 and ***P<0.001 vs. con + mimics control group; $^{\#}$P<0.05, $^{\#\#}$P<0.01 and $^{\#\#\#}$P<0.001 vs. ox-LDL40 + mimics control group; $^{\&}$P<0.05 and $^{\&\&}$P<0.01 vs. con + miR-129-5p mimics group. miR, microRNA; ox-LDL, oxidized low-density lipoprotein; con, control.

is associated with AS, and is formed as a result of ox-LDL oxidation (32-34). In addition, further research has focused on improving and preventing the development of AS. The role of ox-LDL in hyperlipidemia has also been demonstrated as a key risk factor in the development of AS (35). Moreover, the pharmacological inhibition of miRNAs is being used as treatment for a number of human diseases, and ongoing research has focused on the development of RNA-based therapeutics for clinical applications, such as for the treatment of CVD (36). As one of the most important cells in the arterial mesangium, VSMCs serve a key role in the formation of AS through excessive proliferation (37,38). A number of studies have used VSMCs as models to elucidate the pathological mechanism underlying AS. Furthermore, miRNAs have become an integral part in determining the mechanisms associated with AS, and have the potential to act as biomarkers (39,40). Ruan *et al* (41) demonstrated that miR-155 overexpression inhibited apoptosis in different cells including vascular endothelial cells and vascular smooth muscle cells by suppressing the expression of p85α to block Akt activation, which supports a potential therapeutic role in AS. Thus, it was hypothesized that miRNA may regulate the proliferation, migration and cell viability of A7r5 cells induced by ox-LDL.

To understand the functional mechanisms underlying miRNAs, the identification of potential targets involved in their regulation is required. Luo *et al* (42) reported that miR-129-5p attenuates irradiation-induced autophagy and decreases the radio-resistance of breast cancer cells by targeting HMGB1 (42,43). In the present study, the role of miR-129-5p on AS, and the potential underlying molecular mechanisms were investigated. The effects of miR-129-5p on

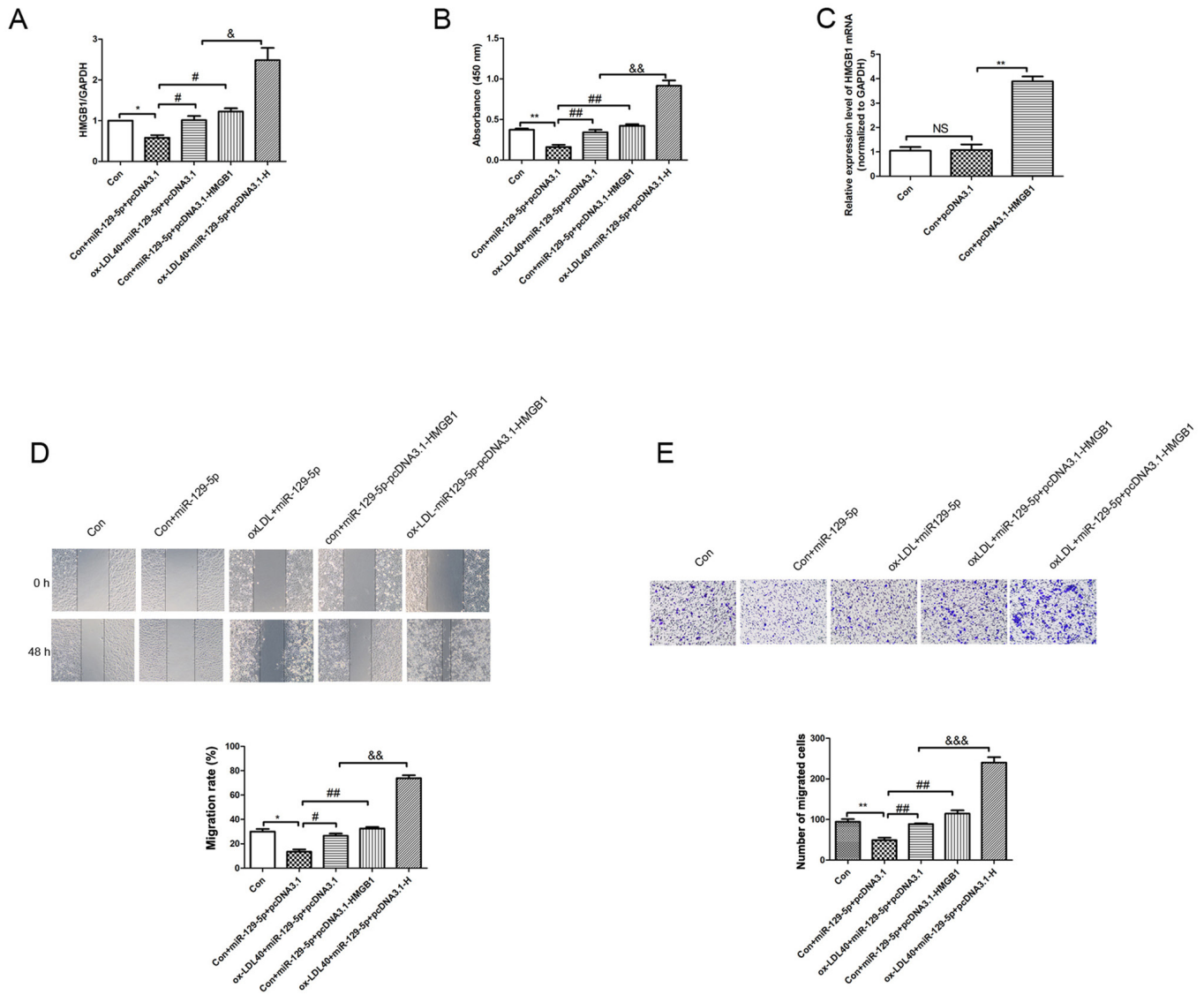

Figure 5. HMGB1 overexpression reverses the miR-129-5p-mediated inhibition of ox-LDL-induced A7r5 cell proliferation and migration. (A) RT-qPCR assays were used to determine the mRNA expression levels of HMGB1 in A7r5 cells. The following groups were established: Control group, con + miR129-5p + pcDNA3.1, 40 μg/ml ox-LDL + miR129-5p + pcDNA3.1, con + miR-129-5p + pcDNA3.1-HMGB1 and 40 μg/ml ox-LDL + miR129-5p + pcDNA3.1-HMGB1. (B) Cell Counting Kit-8 assays were used to determine the effects of ox-LDL treatment on A7r5 cell viability. (C) RT-qPCR analysis was used to detect the mRNA expression level of HMGB1. (D) Wound closure of cells was detected using wound healing assays (magnification, x100). (E) Migration of cells was determined using Transwell assays (magnification, x100). Experiments were repeated three times. *P<0.05, **P<0.01 vs. control group; $^{\#}$P<0.05 and $^{\#\#}$P<0.01 vs. con + miR-129-5p + pcDNA3.1 group; $^{\&}$P<0.05, $^{\&\&}$P<0.01 and $^{\&\&\&}$P<0.05 vs. ox-LDL40 + miR-129-5p + pcDNA3.1 group. HMGB1, high-mobility group box 1 protein; miR, microRNA; ox-LDL, oxidized low-density lipoprotein; con, control; RT-qPCR, reverse transcription-quantitative PCR; NS, non-significant.

the viability and migration of A7r5 cells induced by ox-LDL were also investigated. HMGB1 is a well-established target of the of PI3k/Akt signaling pathway. Moreover, the results of the present study demonstrated that miR-129-5p regulated the PI3k/Akt signaling pathway by targeting HMGB1. Thus, the results of the present study identified HMGB1 as a direct functional target of miR-129-5p in A7r5 cells, and also an important regulator of the PI3k/Akt signaling pathway in VSMCs. For example, the results of the present study demonstrated that the 3'UTR of HMGB1 contained a binding site that matched the miR-129-5p seed sequence. Furthermore, compared with control group, overexpression of miR-129-5p decreased the luciferase activity upstream of the WT 3'UTR of HMGB1, whereas a site mutation in miR-129-5p abolished miR-129-5p regulation. Inhibition of miR-129-5p led to an increase in luciferase activity of WT HMGB1 3'UTR in A7r5 cells. Finally, transfection of the miR-129-5p inhibitor into A7r5 cells suppressed HMGB1 expression levels. Thus, the results of the present study demonstrated that miR-129-5p regulated HMGB1 expression by directly binding to its 3'UTR.

Previous studies (44,45) have indicated the potential roles of HMGB1 in VSMCs. HMGB1 serves a role in the regulation of the PI3k/Akt signaling pathway (44), which is crucial for the development or progression of AS in a number of ways, such as cell growth, migration and apoptosis of A7r5 cells induced by ox-LDL. The effective inhibition of VSMC proliferation at the early stage of AS formation is an important method for the prevention and treatment of vascular hyperplastic lesions and restenosis after angioplasty (46).

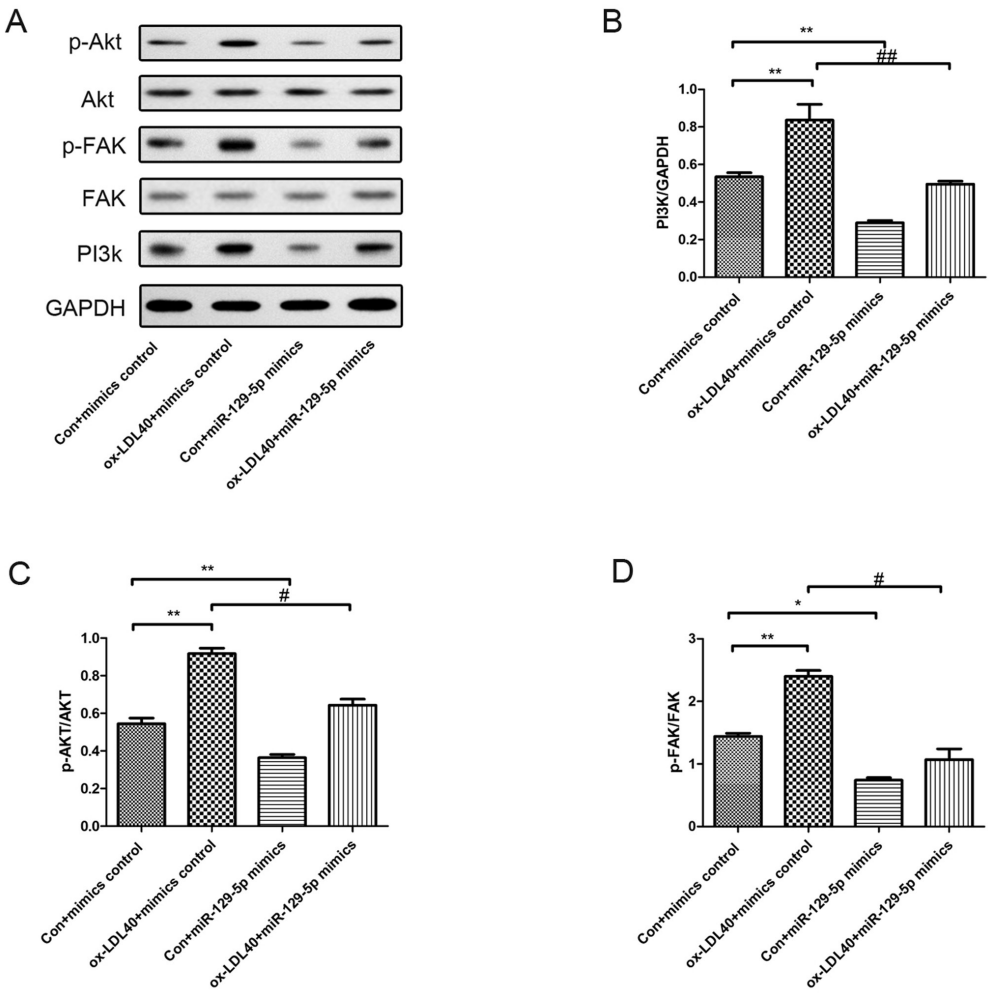

Figure 6. Effects of miR-129-5p on PI3k, p-FAK and p-Akt protein expression levels. Western blot analyses were conducted to determine the phosphorylation levels of FAK and Akt, and the protein expression levels of PI3k. (A) Protein expression levels in A7r5 cells transfected with mimics, 40 μg/ml ox-LDL + mimics control group, miR-129-5p + mimics control group, and 40 μg/ml ox-LDL + miR-129-5p mimics group. Quantification of protein expression levels of (B) PI3k, (C) p-Akt and (D) p-FAK. Experiments were repeated three times. *P<0.05 and **P<0.01 vs. con + mimics control group; $^{\#}$P<0.05 and $^{\#\#}$P<0.01 vs. ox-LDL40 + mimics control group. miR, microRNA; p-, phosphorylated; FAK, focal adhesion kinase; ox-LDL, oxidized low-density lipoprotein; con, control.

In conclusion, miR-129-5p mediated HMGB1 to regulate the PI3k/Akt signaling pathway and further inhibited the proliferation and migration of A7r5 cells induced by ox-LDL. Thus, the present study may provide new insights into the treatment of AS through the regulation of VSMC proliferation and migration.

However, the present study was limited in that it primarily focused on the viability, migration and apoptosis of ox-LDL-induced A7r5 cells. For example, despite there being discussions surrounding the pathological mechanisms underlying the atherosclerotic cell model, these were not verified using any *in vivo* experimental data. In addition, agonists or inhibitors were not used in the present study to explore the signaling pathway. Thus, Akt inhibitors, such as MK2206, should be used in future investigations to further explore the role of the PI3k/Akt signaling pathway regulated by miR-129-5p in CVD.

Acknowledgements

Not applicable.

Funding

The present study was supported by the funded project of National Natural Science Foundation of China (grant. no. 8166020210).

Availability of data and materials

The datasets used and/or analyzed during the present study are available from the corresponding author on reasonable request.

Authors' contributions

HJ wrote the manuscript and analyzed the data. RG and YW participated in experimental design, modification, data analysis and submission. RG participated in experiments and literature review. HJ and YW confirm the authenticity of all the raw data. All authors have read and approved the final manuscript.

Ethics approval and consent to participate

Not applicable.

Patient consent for publication

Not applicable.

Competing interests

The authors declare that they have no competing interests.

References

1. Jackson J, Patterson AJ, MacDonald-Wicks L and McEvoy M: The role of inorganic nitrate and nitrite in CVD. Nutr Res Rev 30: 247-264, 2017.
2. Veerbeek JH, Brouwers L, Koster MP, Koenen SV, van Vliet EO, Nikkels PG, Franx A and van Rijn BB: Spiral artery remodeling and maternal cardiovascular risk: The spiral artery remodeling (SPAR) study. J Hypertens 34: 1570-1577, 2016.
3. Sivasinprasasn S, Wikan N, Tocharus J, Chaichompoo W, Suksamrarn A and Tocharus C: Pelargonic acid vanillylamide and rosuvastatin protect against oxidized low-density lipoprotein-induced endothelial dysfunction by inhibiting the NF-κB/NLRP3 pathway and improving cell-cell junctions. Chem Biol Interact 345: 109572, 2021.
4. Groenen AG, Halmos B, Tall AR and Westerterp M: Cholesterol efflux pathways, inflammation, and atherosclerosis. Crit Rev Biochem Mol Biol 56: 426-439, 2021.
5. Valanti EK, Dalakoura-Karagkouni K, Siasos G, Kardassis D, Eliopoulos AG and Sanoudou D: Advances in biological therapies for dyslipidemias and atherosclerosis. Metabolism 116: 154461, 2021.
6. Zhou Z, Subramanian P, Sevilmis G, Globke B, Soehnlein O, Karshovska E, Megens R, Heyll K, Chun J, Saulnier-Blache JS, *et al*: Lipoprotein-derived lysophosphatidic acid promotes atherosclerosis by releasing CXCL1 from the endothelium. Cell Metab 13: 592-600, 2011.
7. Pirillo A, Norata GD and Catapano AL: LOX-1, OxLDL, and atherosclerosis. Mediators Inflamm 2013: 152786, 2013.
8. Yu Q, Chen S, Tang H, Zhang X, Tao R, Yan Z, Shi J, Guo W and Zhang S: Veratric acid alleviates liver ischemia/reperfusion injury by activating the Nrf2 signaling pathway. Int Immunopharmacol 101: 108294, 2021.
9. Gu Y, Xiao ZH, Wu J, Guo M, Lv P and Dou N: Anti-atherosclerotic effect of afrocyclamin A against vascular smooth muscle cells is mediated via p38 MAPK signaling pathway. Cell J 23: 191-198, 2021.
10. Yang Y, Yang L, Liang X and Zhu G: MicroRNA-155 promotes atherosclerosis inflammation via targeting SOCS1. Cell Physiol Biochem 36: 1371-1381, 2015.
11. Toba H, Cortez D, Lindsey ML and Chilton RJ: Applications of miRNA technology for atherosclerosis. Curr Atheroscler Rep 16: 386, 2014.
12. Zhang Z, Pan X, Yang S, Ma A, Wang K, Wang Y, Li T and Liu S: miR-155 promotes ox-LDL-induced autophagy in human umbilical vein endothelial cells. Mediators Inflamm 2017: 9174801, 2017.
13. Arai K, Jin G, Navaratna D and Lo EH: Brain angiogenesis in developmental and pathological processes: Neurovascular injury and angiogenic recovery after stroke. FEBS J 276: 4644-4652, 2009.
14. Geng Z, Xu F and Zhang Y: MiR-129-5p-mediated Beclin-1 suppression inhibits endothelial cell autophagy in atherosclerosis. Am J Transl Res 8: 1886-1894, 2016.
15. Sun X, Icli B, Wara AK, Belkin N, He S, Kobzik L, Hunninghake GM, Vera MP; MICU Registry, Blackwell TS, *et al*: MicroRNA-181b regulates NF-κB-mediated vascular inflammation. J Clin Invest 122: 1973-1990, 2012.
16. Liu X, Cheng Y, Yang J, Xu L and Zhang C: Cell-specific effects of miR-221/222 in vessels: Molecular mechanism and therapeutic application. J Mol Cell Cardiol 52: 245-255, 2012.
17. Xin M, Small EM, Sutherland LB, Qi X, McAnally J, Plato CF, Richardson JA, Bassel-Duby R and Olson EN: MicroRNAs miR-143 and miR-145 modulate cytoskeletal dynamics and responsiveness of smooth muscle cells to injury. Genes Dev 23: 2166-2178, 2009.
18. Liu YR, Chen JJ and Dai M: Paeonol protects rat vascular endothelial cells from ox-LDL-induced injury via downregulating microRNA-21 expression and TNF-α release. Acta Pharmacol Sin 35: 483-488, 2014.
19. Xu C, Shao Y, Xia T, Yang Y, Dai J, Luo L, Zhang X, Sun W, Song H, Xiao B and Guo J: lncRNA-AC130710 targeting by miR-129-5p is upregulated in gastric cancer and associates with poor prognosis. Tumor Biol 35: 9701-9706, 2014.
20. Long XH, Zhou YF, Peng AF, Zhang ZH, Chen XY, Chen WZ, Liu JM, Huang SH and Liu ZL: Demethylation-mediated miR-129-5p up-regulation inhibits malignant phenotype of osteogenic osteosarcoma by targeting Homo sapiens valosin-containing protein (VCP). Tumor Biol 36: 3799-3806, 2015.
21. Feng J, Guo J, Wang JP and Chai BF: MiR-129-5p inhibits proliferation of gastric cancer cells through targeted inhibition on HMGB1 expression. Eur Rev Med Pharmacol Sci 24: 3665-3673, 2020.
22. Pang X, Zhang Y and Zhang S: High-mobility group box 1 is overexpressed in cervical carcinoma and promotes cell invasion and migration. Oncol Rep 37: 831-840, 2017.
23. Wu CY, Zhou ZF, Wang B, Ke ZP, Ge ZC and Zhang XJ: MicroRNA-328 ameliorates oxidized low-density lipoprotein-induced endothelial cells injury through targeting HMGB1 in atherosclerosis. J Cell Biochem, Oct 15, 2018 (Epub ahead of print). doi: 10.1002/jcb.27469.
24. Moreno JA, Sastre C, Madrigal-Matute J, Muñoz-García B, Ortega L, Burkly LC, Egido J, Martín-Ventura JL and Blanco-Colio LM: HMGB1 expression and secretion are increased via TWEAK-Fn14 interaction in atherosclerotic plaques and cultured monocytes. Arterioscler Thromb Vasc Biol 33: 612-620, 2013.
25. Chen Y, Jiang J, Miao H, Chen X, Sun X and Li Y: Hydrogen-rich saline attenuates vascular smooth muscle cell proliferation and neointimal hyperplasia by inhibiting reactive oxygen species production and inactivating the Ras-ERK1/2-MEK1/2 and Akt pathways. Int J Mol Med 31: 597-606, 2013.
26. Xiao S, Zhang D, Liu Z, Jin W, Huang G, Wei Z, Wang D and Deng C: Diabetes-induced glucolipotoxicity impairs wound healing ability of adipose-derived stem cells-through the miR-1248/CITED2/HIF-1α pathway. Aging (Albany NY) 12: 6947-6965, 2020.
27. Livak KJ and Schmittgen TD: Analysis of relative gene expression data using real-time quantitative PCR and the 2(-Delta Delta C(T)) method. Methods 25: 402-408, 2001.
28. Soares AC and Fonseca DA: Cardiovascular diseases: A therapeutic perspective around the clock. Drug Discov Today 25: 1086-1098, 2020.
29. Benjamin EJ, Virani SS, Callaway CW, Chamberlain AM, Chang AR, Cheng S, Chiuve SE, Cushman M, Delling FN, Deo R, *et al*: Heart disease and stroke statistics-2018 update: A report from the american heart association. Circulation 137: e67-e492, 2018.
30. Pastore I, Bolla AM, Montefusco L, Lunati ME, Rossi A, Assi E, Zuccotti GV and Fiorina P: The impact of diabetes mellitus on cardiovascular risk onset in children and adolescents. Int J Mol Sci 21: 4928, 2020.
31. Ezzatvar Y, Izquierdo M, Núñez J, Calatayud J, Ramírez-Vélez R and García-Hermoso A: Cardiorespiratory fitness measured with cardiopulmonary exercise testing and mortality in patients with cardiovascular disease: A systematic review and meta-analysis. J Sport Health Sci 10; 609-619, 2021.
32. Mehta D and Malik AB: Signaling mechanisms regulating endothelial permeability. Physiol Rev 86: 279-367, 2006.
33. Koshman YE, Patel N, Chu M, Iyengar R, Kim T, Ersahin C, Lewis W, Heroux A and Samarel AM: Regulation of connective tissue growth factor gene expression and fibrosis in human heart failure. J Card Fail 19: 283-294, 2013.
34. Soltani A, Argani H, Rahimipour H, Soleimani F, Rahimi F and Kazerouni F: Oxidized LDL: As a risk factor for cardiovascular disease in renal transplantation. J Bras Nefrol 38: 147-152, 2016 (In English, Portuguese).
35. Maiolino G, Rossitto G, Caielli P, Bisogni V, Rossi GP and Calò LA: The role of oxidized low-density lipoproteins in atherosclerosis: The myths and the facts. Mediators Inflamm 2013: 714653, 2013.
36. Chang TY, Tsai WC, Huang TS, Su SH, Chang CY, Ma HY, Wu CH, Yang CY, Lin CH, Huang PH, *et al*: Dysregulation of endothelial colony-forming cell function by a negative feedback loop of circulating miR-146a and -146b in cardiovascular disease patients. PLoS One 12: e0181562, 2017.
37. Li W, Zhi W, Liu F, He Z, Wang X and Niu X: Atractylenolide I restores HO-1 expression and inhibits Ox-LDL-induced VSMCs proliferation, migration and inflammatory responses. Exp Cell Res 353: 26-34, 2017.

38. Zhang L, Cheng H, Yue Y, Li S, Zhang D and He R: H19 knockdown suppresses proliferation and induces apoptosis by regulating miR-148b/WNT/β-catenin in ox-LDL-stimulated vascular smooth muscle cells. J Biomed Sci 25: 11, 2018.
39. Madrigal-Matute J, Rotllan N, Aranda JF and Fernández-Hernando C: MicroRNAs and atherosclerosis. Curr Atheroscler Rep 15: 322, 2013.
40. Florijn BW, Bijkerk R, van der Veer EP and van Zonneveld AJ: Gender and cardiovascular disease: Are sex-biased microRNA networks a driving force behind heart failure with preserved ejection fraction in women? Cardiovasc Res 114: 210-225, 2018.
41. Ruan Z, Chu T, Wu L, Zhang M, Zheng M, Zhang Q, Zhou M and Zhu G: miR-155 inhibits oxidized low-density lipoprotein-induced apoptosis in different cell models by targeting the p85α/AKT pathway. J Physiol Biochem 76: 329-343, 2020.
42. Luo J, Chen J and He L: mir-129-5p attenuates irradiation-induced autophagy and decreases radioresistance of breast cancer cells by targeting HMGB1. Med Sci Monit 21: 4122-4129, 2015.
43. Han JS, Kim K and Lee M: A high mobility group B-1 box A peptide combined with an artery wall binding peptide targets delivery of nucleic acids to smooth muscle cells. J Cell Biochem 107: 163-170, 2009.
44. Lamb FS, Choi H, Miller MR and Stark RJ: TNFα and reactive oxygen signaling in vascular smooth muscle cells in hypertension and atherosclerosis. Am J Hypertens 33: 902-913, 2020.
45. Zhu XS, Zhou HY, Yang F, Zhang HS and Ma KZ: miR-381-3p inhibits high glucose-induced vascular smooth muscle cell proliferation and migration by targeting HMGB1. J Gene Med 23: e3274, 2021.
46. Chen Z, Pan X, Sheng Z, Yan G, Chen L and Ma G: Baicalin suppresses the proliferation and migration of Ox-LDL-VSMCs in atherosclerosis through upregulating miR-126-5p. Biol Pharm Bull 42: 1517-1523, 2019.